Position of the transverse domain wall controlled by magnetic impurities in rectangular magnetic nanowires

D. Toscano, V. A. Ferreira, S. A. Leonel, P. Z. Coura, F. Sato, R. A. Dias, and B. V. Costa

Citation: Journal of Applied Physics **115**, 163906 (2014); doi: 10.1063/1.4872438
View online: http://dx.doi.org/10.1063/1.4872438
View Table of Contents: http://scitation.aip.org/content/aip/journal/jap/115/16?ver=pdfcov
Published by the AIP Publishing

Position of the transverse domain wall controlled by magnetic impurities in rectangular magnetic nanowires

D. Toscano,[1,a)] V. A. Ferreira,[1,b)] S. A. Leonel,[1,c)] P. Z. Coura,[1,d)] F. Sato,[1,e)] R. A. Dias,[1,f)] and B. V. Costa[2,g)]

[1]*Laboratório de Simulação Computacional, Departamento de Física, Universidade Federal de Juiz de Fora, Juiz de Fora, Minas Gerais 36036-330, Brazil*

[2]*Laboratório de Simulação, Departamento de Física, Universidade Federal de Minas Gerais, Belo Horizonte, Minas Gerais 30123-970, Brazil*

(Received 17 February 2014; accepted 7 April 2014; published online 25 April 2014)

We have performed numerical simulations to demonstrate that the domain wall movement can be controlled introducing a distribution of magnetic impurities in a nanowire. In particular, we have considered two identical impurities equidistant from the nanowire width axis. Pinning and scattering sites for the domain wall can be defined by magnetic impurities, consisting of a local variation of the exchange constant. The domain wall motion was induced by application of a magnetic field pulse and our results indicate that it is possible to control the domain wall position. © *2014 AIP Publishing LLC*. [http://dx.doi.org/10.1063/1.4872438]

I. INTRODUCTION

The controlled movement of domain walls in magnetic nanowires is a subject of fundamental importance for the realization of future spintronic devices, used to perform logical operations[1,2] or even to encode information for data storage.[3,4]

A transverse domain wall can be injected into a rectangular nanowire made of a soft magnetic material;[5–7] since the magnetic shape anisotropy predominates over the magnetocrystalline anisotropy, the magnetization of wire is largely aligned along the axis of nanowire length. In this type of domain wall, the magnetization is confined on the plan structure of the strip, and at the boundary between the domains, the magnetization develops a component along the nanowire width (y-axis, see Fig. 1) in which the magnetic moments vary gradually from one domain to another. At the wall, the magnetization can point along $+y$ or $-y$ direction; the polarity of the domain wall is determined by the direction of this magnetization. From the technological point of view, these two-fold degenerated states can be useful to store information, so that a nanowire containing a single transverse domain wall could store one bit of data.

There are two kinds of transverse domain walls which depend on the magnetization orientation between the antiparallel domains; thus, a head-to-head or a tail-to-tail domain wall can be formed. When multiple domain walls are present in the same nanowire, adjacent domain walls alternate between head-to-head and tail-to-tail configurations. When the nanowire presents a pair of domain walls, they interact with each other.[8] Their domain wall polarities define if the interaction will be attractive (parallel polarities) or repulsive (antiparallel polarities).

Domain walls can be manipulated through the application of a magnetic field[9–14] or a spin-polarized current.[15–18] For small or moderate excitations, domain walls behave as quasiparticles restricted to the unidirectional movement. When an external magnetic field is applied along the wire's length to move a single domain wall, the domain with magnetization oriented in the direction of the field expands to minimize the Zeeman energy, and, as a result, the wall is shifted from its equilibrium position. Thus, we can associate dynamic variables with the domain wall, such as position, velocity, and so on. For the movement control of the domain wall, it is very important to determine or even impose critical positions where the domain wall stops. These critical points can be pinning or scattering sites, respectively, corresponding to potential well or potential barrier for the domain wall. The inclusion of well-located confining potentials in the system can be accomplished by different ways. Generally, non-magnetic imperfections which distort locally the wire geometry generate pinning sites. Thus, notches along the edges of the wire have been widely used to trap domain walls.[19–26] We believe that both pinning and scattering sites can be originated from a local modification of the sample magnetic properties. As it has been reported in previous articles,[27–32] magnetic impurities, e.g., localized magnetic modifications obtained by ion irradiation or implantation into magnetic thin films and multilayers have been employed to manipulate and control the magnetization dynamics in nanostructured systems. In this case, no local modification of

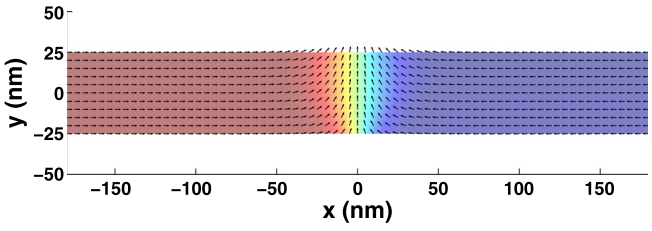

FIG. 1. Schematic view of the nanowire with length L along x-axis, width d along y-axis, and thickness t along z-axis. Initially the transverse domain wall is considered at the geometric center of the wire.

[a)]Electronic mail: danilotoscano@fisica.ufjf.br
[b)]Electronic mail: vanessaferreira@fisica.ufjf.br
[c)]Author to whom correspondence should be addressed. Electronic mail: sidiney@fisica.ufjf.br
[d)]Electronic mail: pablo@fisica.ufjf.br
[e)]Electronic mail: sjfsato@fisica.ufjf.br
[f)]Electronic mail: radias@fisica.ufjf.br
[g)]Electronic mail: bvc@fisica.ufmg.br

system geometry is required. Recently, magnetic soft spots have already been intentionally incorporated in Permalloy nanowires and has been used to induce pinning sites.[33,34] Furthermore, for nanowires with perpendicular magnetic anisotropy, pinning sites can arise from a local reduction of the anisotropy constant.[35] Up to now, there are no experimental results about which possible magnetic impurity could come to act as a scattering center for transverse domain walls. In fact, little or nothing is mentioned about scattering sites and their potential applications in devices involving domain wall movement.

In this paper, we investigate the possibility of using magnetic impurities to control the transverse domain wall position along a rectangular magnetic nanowire. For this purpose, linear arrangements of magnetic impurities have been designed as shown in Figs. 2 and 3. We show that with the usage of linear arrangement of impurities, one can create a two-fold degenerate state in the system, that is, the wall is pinned or blocked in the neighborhood of one of these magnetic impurities. Thus, besides storing one bit in the domain wall polarity, it is possible to store another bit in its position. Consequently, a nanowire containing a single transverse domain wall confined between two identical magnetic impurities could store up to 2 bits of data.

II. MODEL AND METHODOLOGY

In an early study, we have presented a Hamiltonian model describing two types of pointlike magnetic impurities that can behave as pinning or scattering sites for the transverse domain wall in magnetic nanowires.[36] It has been emphasized that a local variation (decrease or increase) of the exchange constant was responsible by emergence of a short-range interaction potential (attractive or repulsive) between the domain wall and the magnetic impurity. We have considered a classical ferromagnet model described by the following Hamiltonian:

$$H = J\Bigg\{ -\frac{1}{2}\sum_{\langle i\neq i',j\rangle} \hat{m}_i\cdot\hat{m}_j - \frac{J'}{2J}\sum_{\langle i',j\rangle}\hat{m}_{i\prime}\cdot\hat{m}_j + \frac{D}{2J}\sum_{i,j}\left[\frac{\hat{m}_i\cdot\hat{m}_j - 3(\hat{m}_i\cdot\hat{r}_{ij})(\hat{m}_j\cdot\hat{r}_{ij})}{(r_{ij}/a)^3}\right] - \frac{Z}{J}\sum_i \hat{m}_i\cdot\vec{b}_i^{\,ext}\Bigg\}, \quad (1)$$

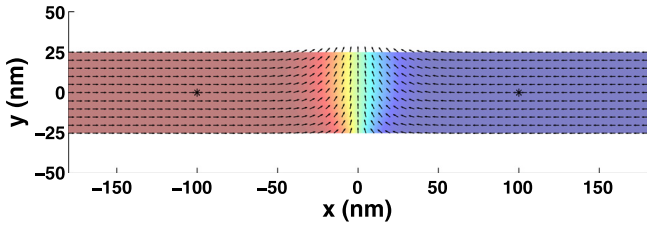

FIG. 2. Schematic view of the modified nanowires. The two black spots represent small clusters containing magnetic impurities located on the wire axis at $y_{imp} = 0$, $x_{imp} = -100$nm, and $x_{imp} = 100$ nm. They can act as pinning or scattering sites for the domain wall.

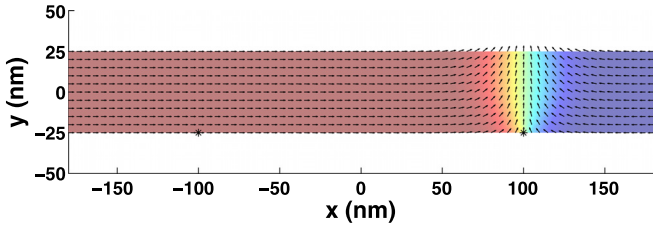

FIG. 3. Schematic view of the modified nanowires. The two black spots represent small clusters containing magnetic impurities located on the wire edge at $y_{imp} = -25$ nm, $x_{imp} = -100$ nm, and $x_{imp} = 100$ nm. They can act as pinning or scattering sites for the domain wall.

where $\hat{m}_k \equiv (m_k^x, m_k^y, m_k^z)$ is a dimensionless vector with $|\hat{m}_k| = 1$ representing the magnetic moment located at the site k of the lattice. The first term in Eq. (1) represents the ferromagnetic coupling only for sites without impurities, whereas the second takes into account the exchange interaction between sites with and without impurities. The exchange interactions between magnetic sites and the one containing the impurity were modeled by ferromagnetic coupling with the exchange constant strength J' differing of its value for sites without impurities J. Thus, we have been describing two possible types of magnetic impurities, acting as pinning $(J'/J < 1)$ or scattering $(J'/J > 1)$ sites for the domain wall. The following terms are dimensionless versions of dipolar and Zeeman interactions, respectively. The Hamiltonian (1) can be rewritten as $H = J\mathcal{H}$, where $\mathcal{H}$ is the dimensionless term in curly brackets. The system energy is measured in unities of J.

In the simulations, we have been developing and using our own numerical code written in Fortran 90 programming language. The dynamics of the system is followed by solving numerically the discrete version of the Landau-Lifshitz-Gilbert equation given by

$$\frac{d\hat{m}_i}{d\tau} = -\frac{1}{1+\alpha^2}[\hat{m}_i\times\vec{b}_i + \alpha\,\hat{m}_i\times(\hat{m}_i\times\vec{b}_i)], \quad (2)$$

where $\vec{b}_i = -\frac{\partial\mathcal{H}}{\partial\hat{m}_i}$ is the dimensionless effective field at site i containing individual contributions from the exchange, dipolar, and Zeeman fields.

In the micromagnetics approach, the interactions constants depend on the material parameters and also the manner in which the system is partitioned into cells. As in Refs. 37–39, we have chosen to use cubic cells of edge length a. In this case, the interactions constants between the cells are given by $J = 2Aa$ and $\frac{D}{J} = \frac{1}{4\pi}\left(\frac{a}{\lambda}\right)^2$. If there is an external magnetic field, the coefficient of Zeeman interaction is $\frac{Z}{J} = \left(\frac{a}{\lambda}\right)^2$. We have used the typical parameters for Permalloy-79: the saturation magnetization $M_S = 8.6\times10^5$ A/m, the exchange stiffness constant $A = 1.3\times10^{-11}$ J/m, and the damping constant $\alpha = 0.01$. Using these parameters, we have estimated the exchange length as $\lambda = \sqrt{\frac{2A}{\mu_0 M_S^2}} \approx 5.3$ nm and the unit cell size was chosen as $5\times5\times5$ nm^3. The time t is obtained by $t = \tau/\omega_0$, where τ is the dimensionless simulation time and $\omega_0 = \left(\frac{\lambda}{a}\right)^2\mu_0\gamma M_s$. The equations of motion (2) were integrated forward by using the fourth-order predictor-corrector scheme with time step $\Delta\tau = 0.01$.

In our simulations, we have used the nanowires with length $L = 1\,\mu$m, width $d = 50$ nm and thickness $t = 5$ nm, differing one to another only in the magnetic impurities arrangement parameters: the local variation of the exchange constant J'/J and its position $(\pm x_{imp}, y_{imp})$. For a local reduction of the exchange constant, we have considered five different values, $J'/J = 0.3$, 0.4, 0.5, 0.6, and 0.7, whereas for a local increase of the exchange constant, we have used $J'/J = 1.3$, 1.5, 1.7, 2.0, and 3.0. The adopted coordinate system is shown in Fig. 1. The impurity coordinate parallel to the wire axis (x-axis) was fixed $x_{imp} = \pm 100$ nm and the two impurities were assumed to be identical, that is, we have considered the same value for J'/J. For the coordinate y_{imp}, we have considered two situations. One of them, due to symmetry, the pair of impurities was placed exactly on the wire axis, $y_{imp} = 0$ (see Fig. 2). In the other, they were strategically located on the wire edge, in particular, the one where the magnetic moments of the wall point toward the inside of the wire, $y_{imp} = -25$ nm (see Fig. 3), because the strength of the pinning and scattering is maximized in this case as it has been addressed in Ref. 36.

In order to obtain the remanent states of the nanowires, we have chosen, as initial condition, the system with a single transverse domain wall in the head-to-head structure placed exactly at the middle of the two magnetic impurities (see, for example, Fig. 2). The integration of the equations of motion (2) at zero external magnetic field, $\vec{b}_i^{ext} = \vec{0}$, leads the system to a local energy minimum configuration, and we assumed that the nanowire remanent state was reached. Due to the arrangement of impurities to be symmetric, the domain wall stays at the geometric center of the wire. To study the effect of pinning and scattering, the domain wall motion was induced by the application of a low magnetic field pulse in order to move the wall toward the impurity on the right. Thus, the domain wall found a new equilibrium position in the neighborhood of the impurity (see, for example, Fig. 3). The equilibrium configurations obtained in this way were saved and used as initial configurations in other experiments where the field was applied in both directions along the x-axis.

Over a wide range of the excitation amplitudes B and exchange constant ratio J'/J, we numerically calculated the dynamic response of the wall under the influence of a homogeneous magnetic field pulse given by $\vec{B}_i^{ext} = B\,\hat{x}$. In all simulations, the duration of the pulse was always the same, $\Delta t = 0.5$ ns. The relation between the applied magnetic field and its dimensionless correspondent is $\vec{B}_i^{ext} = \mu_0 M_S\, \vec{b}_i^{ext}$.

III. RESULTS AND DISCUSSIONS

Figs. 4 and 5 are event diagrams showing the dynamics behavior of the wall under the influence of the field pulse. In Figs. 4 and 5, the sub-figures (a) and (c) represent the situation where the impurities were located on the wire axis and sub-figures (b) and (d) represent the situation where the impurities were located on the wire edge. In sub-figures (a) and (b), the magnetic field was applied in the negative direction of the x-axis, whereas in sub-figures (c) and (d), it was applied in the opposite direction (in the positive direction of the x-axis). From Figs. 4 and 5, we can observe the occurrence of some events, which are indicated in their captions.

Analyzing Fig. 4, it can be noted that there is a depinning field, which is the minimum value of the applied field required for the domain wall escapes from the potential well created by the pinning impurity. Below this minimum value, the domain wall remains pinned to the impurity. The magnitude of the depinning field depends not only on the reduction of the exchange constant but also on the impurities location. It is possible to observe that pinning effects are stronger when the impurities are on the wire's edge, in particular, that one where domain wall is narrower. This observation is in agreement with the results presented in our recent work.[36] In that work, due to the fact that the domain wall is asymmetric with respect to the y-axis (see Fig. 1), we demonstrated that when the impurity is located on the wire edge where

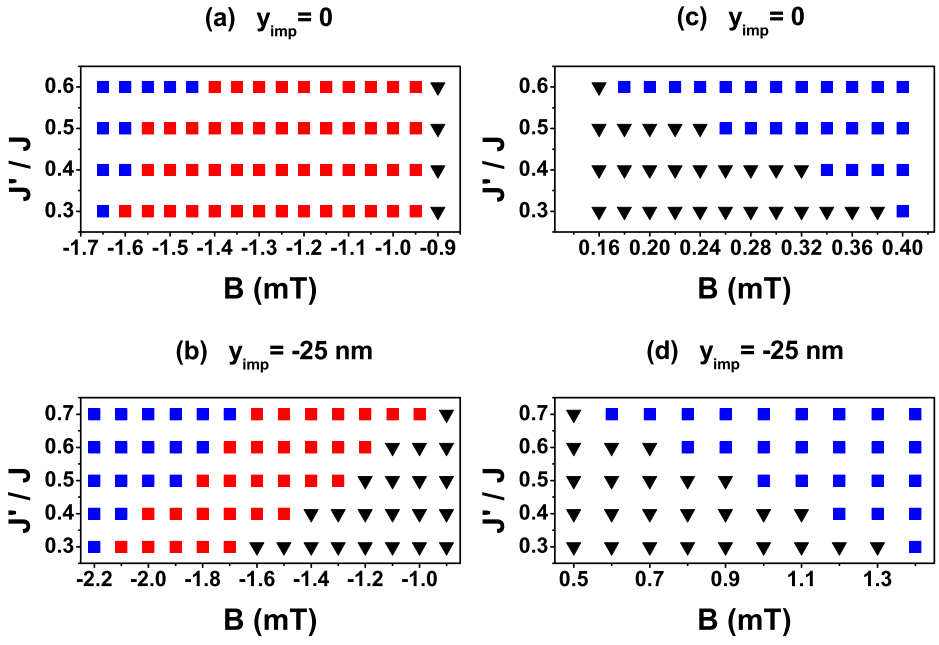

FIG. 4. Position controllability diagrams of the domain wall using a pair of magnetic impurities acting as pinning sites. Black triangles correspond to a combination of parameters for which the wall remained trapped to the impurity on the right. Red squares correspond to the events in which the domain wall position could be controlled, that is, after applying the magnetic field pulse, the wall was moved toward the impurity on the left and was captured by it (see the video in the supplementary material[40] labeled S1). Blue squares correspond to the events where the wall was depinned from the impurity on the right and was expulsed.

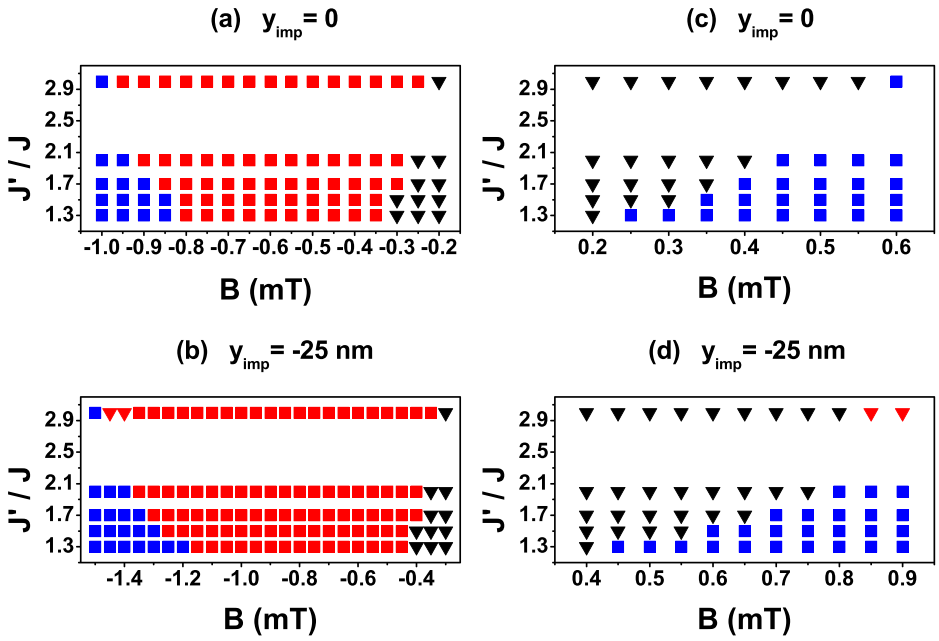

FIG. 5. Position controllability diagrams of the domain wall using a pair of magnetic impurities acting as scattering sites. Black triangles correspond to a combination of parameters for which the wall remained on its equilibrium position near the impurity on the right. Red squares correspond to the events in which the domain wall position could be controlled, that is, after applying the magnetic field pulse, the wall was moved toward the impurity on the left and was blocked by it (see the video in the supplementary material[40] labeled S2). Red triangles correspond to a combination of parameters for which the wall stopped on its equilibrium position near the impurity on the left. Blue squares correspond to the events where the wall was not blocked by the impurities and was expulsed.

head-to-head domain wall is narrower, the strength of the pinning and scattering are maximized. For excitation amplitudes strong enough above the depinning field, the wall can escape from the potential well created by the impurity, and it can result in the wall expulsion or wall capture by the second impurity, depending on the direction of the applied field.

The diagrams of Fig. 5 are similar to the diagrams of Fig. 4 except that the impurities represent potential barriers for the domain wall. By analyzing Figs. 5(c) and 5(d), one can observe that there is a deblocking field which is the minimum value of the applied field required for the domain wall that overcomes the potential barrier created by the scattering impurity. Below this minimum value, the domain wall remains blocked by the impurity. The magnitude of the deblocking field depends not only on the increase of the exchange constant but also on the impurities location, for the same reasons explained above. For excitation amplitudes strong enough above the deblocking field, the wall can overcome the potential barrier created by the impurity, and it can result in the wall expulsion or wall blocking by the second impurity, depending on the direction of the applied field.

Since we know the depinning or deblocking fields, it is possible to control the domain wall position in modified nanowires. The control of the domain wall position occurs in a certain range of the parameters involving the tuning of the excitation amplitude and the depth (height) of the potential well (barrier) (see, for example, the supplemental videos S1 and S2 in Ref. 40).

Furthermore, it was observed in our simulations that tail-to-tail domain wall is asymmetric with respect to the y-axis and is narrower on one of the wire edges. Although in this work we considered the head-to-head domain wall, we found that for both types of wall and chirality, if we strategically inserted the magnetic impurities on the wire edge where the domain wall is narrower, the strength of the pinning and scattering will be maximized. Consequently, one can also control the position of the tail-to-tail domain wall with the same parameters used to control the position of the head-to-head domain wall (see, for example, videos S3 and S4 in Ref. 40).

In summary, we have demonstrated by computational simulation that dynamics of the transverse domain wall in a rectangular magnetic nanowire can be controlled introducing a distribution of magnetic impurities in the system. The magnetic impurities consisting of a local variation of the exchange stiffness constant can represent locally a potential well or a potential barrier for the domain wall. The usage of a linear arrangement of impurities consisting of a pair of identical magnetic impurities has been proposed to stabilize the domain wall motion. By imposing very well defined positions along the wire (pinning or scattering sites), we can control the domain wall position. Although the results presented here are for a very simple distribution of magnetic impurities, we believe their consequences can be planned and extended for the realization of future spintronic devices based on magnetic domain walls.

ACKNOWLEDGMENTS

This work was partially supported by CNPq and FAPEMIG (Brazilian Agencies). Numerical works were done at the Laboratório de Simulação Computacional do Departamento de Física da UFJF. We would like to thank our friend Dr. Wilson Oliveira, who is no more for pleasant coexistence and friendship in these 24 years in the Departamento de Física da UFJF.

[1]D. A. Allwood, G. Xiong, C. C. Faulkner, D. Atkinson, D. Petit, and R. P. Cowburn, Science **309**, 1688–1692 (2005).
[2]K. Nagai, Y. Cao, T. Tanaka, and K. Matsuyama, J. Appl. Phys. **111**, 07D130 (2012).
[3]S. S. P. Parkin, M. Hayashi, and L. Thomas, Science **320**, 190–194 (2008).
[4]M. Hayashi, L. Thomas, R. Moriya, C. Rettner, and S. S. P. Parkin, Science **320**, 209–211 (2008).
[5]R. P. Cowburn, D. A. Allwood, G. Xiong, and M. D. Cooke, J. Appl. Phys. **91**, 6949–6951 (2002).

[6]A. Himeno, T. Ono, S. Nasu, K. Shigeto, K. Mibu, and T. Shinjo, J. Appl. Phys. **93**, 8430–8432 (2003).
[7]M. Hayashi, L. Thomas, Ya. B. Bazaliy, C. Rettner, R. Moriya, X. Jiang, and S. S. P. Parkin, Phys. Rev. Lett. **96**, 197207 (2006).
[8]A. Kunz and E. W. Rentsch, IEEE Trans. Magn. **46**, 1556–1558 (2010).
[9]T. Ono, K. Shigeto, K. Mibu, N. Hosoito, and T. Shinjo, Science **284**, 468–470 (1999).
[10]D. Atkinson, D. A. Allwood, G. Xiong, M. D. Cooke, C. C. Faulkner, and R. P. Cowburn, Nature Mater. **2**, 85–87 (2003).
[11]Y. Nakatani, A. Thiaville, and J. Miltat, Nature Mater. **2**, 521–523 (2003).
[12]G. S. D. Beach, C. Nistor, C. Knutson, M. Tsoi, and J. L. Erskine, Nature Mater. **4**, 741–744 (2005).
[13]C.-Y. You, Appl. Phys. Lett. **92**, 192514 (2008).
[14]M. Vázquez, G. A. Basheed, G. Infante, and R. P. D. Real, Phys. Rev. Lett. **108**, 037201 (2012).
[15]L. Berger, J. Appl. Phys. **49**, 2156–2161 (1978).
[16]A. Yamaguchi, T. Ono, S. Nasu, K. Miyake, K. Mibu, and T. Shinjo, Phys. Rev. Lett. **92**, 077205 (2004).
[17]M. Hayashi, L. Thomas, C. Rettner, R. Moriya, Y. B. Bazaly, and S. S. P. Parkin, Phys. Rev. Lett. **98**, 037204 (2007).
[18]G. S. D. Beach, M. Tsoi, and J. L. Erskine, J. Magn. Magn. Mater. **320**, 1272–1281 (2008).
[19]C. K. Lim, T. Devolder, C. Chappert, J. Grollier, V. Cros, A. Vaurès, A. Fert, and G. Faini, Appl. Phys. Lett. **84**, 2820–2822 (2004).
[20]M. Kläui, H. Ehrke, U. Rüdiger, T. Kasama, R. E. Dunin-Borkowski, D. Backes, L. J. Heyderman, C. A. F. Vaz, J. A. C. Bland, G. Faini, E. Cambril, and W. Wernsdorfer, Appl. Phys. Lett. **87**, 102509 (2005).
[21]L. Thomas, M. Hayashi, X. Jiang, R. Moriya, C. Rettner, and S. S. P. Parkin, Nature (London) **443**, 197–200 (2006).
[22]M. Hayashi, L. Thomas, C. Rettner, R. Moriya, X. Jiang, and S. S. P. Parkin, Phys. Rev. Lett. **97**, 207205 (2006).
[23]M. Hayashi, L. Thomas, C. Rettner, R. Moriya, and S. S. P. Parkin, Appl. Phys. Lett. **92**, 162503 (2008).
[24]L. K. Bogart, D. Atkinson, K. O'Shea, D. McGrouther, and S. McVitie, Phys. Rev. B **79**, 054414 (2009).
[25]M.-Y. Im, L. Bocklage, P. Fischer, and G. Meier, Phys. Rev. Lett. **102**, 147204 (2009).
[26]D. Djuhana, H.-G. Piao, S-H. Lee, D.-H. Kim, S.-M. Ahn, and S.-B. Choe, Appl. Phys. Lett. **97**, 022511 (2010).
[27]C. Chappert, H. Bernas, J. Ferre, V. Kottler, J.-P. Jamet, Y. Chen, E. Cambril, T. Devolder, F. Rousseaux, V. Mathet, and H. Launois, Science **280**, 1919–1922 (1998).
[28]L. D. Ozkaya, R. M. Langford, W. L. Chan, and A. K. Petford-Long, J. Appl. Phys. **91**, 9937–9942 (2002).
[29]L. Folks, R. E. Fontana, B. A. Gurney, J. R. Childress, S. Maat, J. A. Katine, J. E. E. Baglin, and A. J. Kelloc, J. Phys. D: Appl. Phys. **36**, 2601–2604 (2003).
[30]J. Fassbender, J. von Borany, A. Mücklich, K. Potzger, W. Möller, J. McCord, L. Schultz, and R. Mattheis, Phys. Rev. B **73**, 184410 (2006).
[31]J. Fassbender and J. McCord, J. Magn. Magn. Mater. **320**, 579–596 (2008).
[32]J. Fassbender, T. Strache, M. O. Liedke, D. Markó, S. Wintz, K. Lenz, A. Keller, S. Facsko, I. Mönch, and J. McCord, New J. Phys. **11**, 125002 (2009).
[33]A. Vogel, S. Wintz, T. Gerhardt, L. Bocklage, T. Strache, M.-Y. Im, P. Fisher, J. Fassbender, J. McCord, and G. Meier, Appl. Phys. Lett. **98**, 202501 (2011).
[34]M. A. Basith, S. McVitie, D. McGrouther, and J. N. Chapman, Appl. Phys. Lett. **100**, 232402 (2012).
[35]T. Gerhardt, A. Drews, and G. Meier, J. Phys.: Condens. Matter **24**, 024208 (2012).
[36]V. A. Ferreira, D. Toscano, S. A. Leonel, P. Z. Coura, R. A. Dias, and F. Sato, J. Appl. Phys. **114**, 013907 (2013).
[37]D. Toscano, S. A. Leonel, R. A. Dias, P. Z. Coura, and B. V. Costa, J. Appl. Phys. **109**, 076104 (2011).
[38]J. H. Silva, D. Toscano, F. Sato, P. Z. Coura, B. V. Costa, and S. A. Leonel, J. Magn. Magn. Mater. **324**, 3083–3086 (2012).
[39]D. Toscano, S. A. Leonel, P. Z. Coura, F. Sato, R. A. Dias, and B. V. Costa, Appl. Phys. Lett. **101**, 252402 (2012).
[40]See the supplementary material at http://dx.doi.org/10.1063/1.4872438 for videos of the following: video S1 shows the control of the head-to-head domain wall position using a pair of magnetic impurities acting as pinning sites. In this simulation, we have used $J'/J = 0.5$ and excitation amplitude $B = 1.60$ mT. Initially, the field pulse was applied in the negative direction of the x-axis. After the wall is captured by the impurity on the left, the field pulse was applied in the opposite direction, and so on. Video S2 shows the control of the head-to-head domain wall position using a pair of magnetic impurities acting as scattering sites. In this simulation, we have used $J'/J = 1.5$ and excitation amplitude $B = 1.15$ mT. Initially, the field pulse was applied in the negative direction of the x-axis. After the wall is blocked by the impurity on the left, the field pulse was applied in the opposite direction, and so on. Video S3 shows the control of the tail-to-tail domain wall position using a pair of magnetic impurities acting as pinning sites. In this simulation, we have used $J'/J = 0.5$ and excitation amplitude $B = 1.60$ mT. Initially, the field pulse was applied in the negative direction of the x-axis. After the wall is captured by the impurity on the left, the field pulse was applied in the opposite direction, and so on. Video S4 shows the control of the tail-to-tail domain wall position using a pair of magnetic impurities acting as scattering sites. In this simulation, we have used $J'/J = 1.5$ and excitation amplitude $B = 1.15$ mT. Initially, the field pulse was applied in the negative direction of the x-axis. After the wall is blocked by the impurity on the left, the field pulse was applied in the opposite direction, and so on.